APPENDIX B

PRETEST FUEL ROD CHARACTERIZATION

APPENDIX B

PRETEST FUEL ROD CHARACTERIZATION

The pretest characterization of the four Test RIA 1-1 fuel rods and flow shrouds is presented in this appendix. The test rods were selected from 68 irradiated MAPI[a] rods and 35 unirradiated Saxton rods. The preirradiation characterization provides referential information for use in analytical models and for posttest comparison.

1. FUEL ROD DESIGN

The test fuel rods contained a 0.914-m-long fuel stack composed of 60 ceramic fuel pellets [nominally 94% theoretical density, 5.7 wt% (irradiated) and 5.8 wt% (unirradiated), enriched UO_2], each nominally 8.5 mm in diameter and 15.2 mm long. The fuel pellets were contained in a zircaloy-4 cladding tube of nominally 9.9-mm outside diameter, and 0.62- (irradiated) and 0.53-mm (unirradiated) wall thicknesses. The nominal fuel-cladding diametral gap was 0.828 mm for the previously irradiated rods and 0.867 mm for the previously unirradiated rods.

Five test fuel rods were used in Test RIA 1-1. Two MAPI fuel rods, previously irradiated to a burnup of approximately 4600 MWd/tU (0.49 at.%) in the Saxton reactor were selected for use in the test.[B-1] Three previously unirradiated fuel rods were also used in the test and were built by EG&G Idaho, Inc., using cladding provided to the U.S. Department of Energy by Westinghouse Electric Corporation. The two irradiated rods were designated Rods 801-1 and 801-2, and the three previously unirradiated rods were designated Rods 801-3, 801-4, and 801-5. Previously unirradiated Rod 801-4 was removed from the test assembly after the power calibration and preconditioning phases of the test were completed, and was replaced prior to the

---

a. The MAPI rods were built by Westinghouse Electric Co., and irradiated in the Saxton reactor for the Mitsubishi Atomic Power Industries, Inc., Tokyo, Japan.

test power burst with Rod 801-5. Rod 801-5, which experienced only the test power burst, was used for the radiochemical determination of burnup to calculate the energy produced. The rod designations and prior irradiation history are summarized in Table B-1. The nominal design characteristics of these rods are listed in Table B-2.

Table B-1. Test RIA 1-1 fuel rod designations and burnup

Test RIA 1-1 Rod Identification	Westinghouse Electric Company Correspondiug Rod Identification	Average Burnup (MWd/tU)
801-1	M-42	4600
801-2	M-9	4650
801-3	958	Unirradiated
801-4	951	Unirradiated
801-5	950	Unirradiated

The cladding inside diameters were measured at angular orientations of 0 and 90 degrees, at increments of 25.4 mm on each of the three previously unirradiated fuel rods. The cladding outside diameters were measured at two angular orientations (0 and 90 degrees) at elevations of 0.025, 0.304, 0.609, and 0.914 m above the bottom of the cladding tube. The cladding inside diameter measurements were made with an air gage (accuracy ± 2.5 µm), and the cladding outside diameter measurements were made using a micrometer (accuracy ± 0.03 mm). These measurements are presented for the three previously unirradiated rods (801-3, 801-4, and 801-5) in Tables B-3, B-4, and B-5, respectively.

The unirradiated Saxton rods used in the test were modified by exchanging the original unirradiated 9.5 wt% enriched fuel pellets with 5.8 wt% enriched pellets fabricated by Battelle Pacific Northwest Laboratory (PNL). The physical dimensions (diameter, length, weight, and density) of the 60 UO_2 fuel pellets comprising the fuel columns of the previously unirradiated fuel rods (801-3, and 801-5) are presented in Tables B-6 and B-7, respectively. The UO_2 pellet data contained in these tables were obtained by measuring the length between the upper and lower

Table B-2. Test RIA 1-1 fuel rod component nominal design data

Characteristics	MAPI[a]	Unirradiated		
	801-1, -2	801-3	801-4	801-5
Fuel[b]				
Enrichment (wt% ^{235}U of total U)	5.7	5.8	5.8	5.8
Fabricated fuel density (% TD)	94	94.5	94.5	94.5
Original pellet diameter (mm)	8.59	8.53	8.53	8.53
Original pellet length (mm)	15.2	15.2	15.2	15.2
Dish depth (mm)	0.33	0.33	0.33	0.33
Fuel stack length (m)	0.914	0.914	0.914	0.914
Burnup (MWd/tU)	4600	--	--	--
Cladding[c]				
Outside diameter (mm)	9.995	9.93	9.93	9.93
Wall thickness (mm)	0.622	0.533	0.533	0.533
Inside diameter (mm)	8.75	8.864	8.864	8.864
Yield strength (0.2% offset, MPa)	570	570	570	570
Tensile (ultimate) strength (MPa)	700	700	700	700
Elongation (%)	18	18	18	18
Hardness (R_B)	100	100	100	100
End Cap Rod Stock[d]				
Yield strength (0.2% offset, MPa)	241	241	241	241
Tensile strength (MPa)	413	413	413	413
Elongation (%)	14	14	14	14
Hardness (BHN)	180	180	180	180
Compression Springs[e]				
Wire diameter (mm)	1.018	1.018	1.018	1.018
Tensile strength (MPa)	162	162	162	162
Spring outside diameter (mm)	8.382	8.382	8.382	8.382
Free length (mm)	54.788	54.788	54.788	54.788
Total number of coils	17	17	17	17

Table B-2. (continued)

Characteristics	MAPI[a] 801-1, -2	Unirradiated 801-3	Unirradiated 801-4	Unirradiated 801-5
Fuel Rod				
Insulators	None	None	None	None
Gas plenum length (mm)	45.7	45.7	45.7	45.7
Measured void volume (10^{-2} m^3)	6	8.2	5.7	5.6
Initial fill gas pressure (MPa)	f	--	--	--
Fill gas for PBF test	g	h	h	h
Fill gas pressure for PBF test (MPa)	0.103	0.103	0.103	0.103
Fuel-cladding gap (diametral mm)	0.26	0.33	0.33	0.33
Overall rod length (m)	1.087 1.072	1.072	1.068	1.068

a. Data are preirradiation values.

b. Ceramic, dished and sintered, uranium dioxide pellets.

c. Zircaloy-4 alloy cladding, as-received (50% cold worked) and stress relieved.

d. Zircaloy-2 alloy manufactured to ASTM Standard B 351-67, Grade RA-1 (annealed): Rods 801-1, 801-3, 801-4, and 801-5 only.

e. Oil-tempered, chromium-vanadium alloy spring steel manufactured to ASTM Standard A 231-68; Rods 801-3, 801-4, and 801-5 only.

f. Air fill gas at 0.103 MPa.

g. 77.7% He/22.3% Ar fill gas.

h. Commercially pure helium gas (nominally 99.995% pure helium).

Table B-3. Cladding inside and outside diameter data for Rod 801-3

Distance from Bottom of Cladding (m)	Cladding Inside Diameter (mm)		Cladding Outside Diameter (mm)	
	0°	90°	0°	90°
0.0254	8.7427	8.7516	9.9151	9.9139
0.0508	8.7462	8.7579	9.9172	9.9190
0.0762	8.7488	8.7483	9.9294	9.9296
0.1016	8.7490	8.7462	9.9291	9.9294
0.1270	8.7488	8.7473	9.9281	9.9296
0.1524	8.7475	8.7475	9.9296	9.9284
0.1778	8.7465	8.7457	9.9286	9.9281
0.2032	8.7450	8.7457	9.9286	9.9266
0.2286	8.7450	8.7473	9.9281	9.9276
0.2540	8.7432	8.7475	9.9284	9.9258
0.2794	8.7432	8.7475	9.9291	9.9256
0.3048	8.7427	8.7467	9.9291	9.9273
0.3302	8.7422	8.7467	9.9286	9.9258
0.3556	8.7412	8.7465	9.9299	9.9256
0.3810	8.7499	8.7460	9.9291	9.9258
0.4064	8.7406	8.7460	9.9296	9.9263
0.4318	8.7399	8.7442	9.9286	9.9271
0.4572	8.7434	8.7473	9.9278	9.9263
0.4826	8.7389	8.7473	9.9268	9.9261
0.5080	8.7391	8.7457	9.9268	9.9251
0.5334	8.7404	8.7478	9.9268	9.9256
0.5588	8.7406	8.7424	9.9266	9.9266
0.5842	8.7419	8.7429	9.9271	9.9258
0.6096	8.7386	8.7406	9.9271	9.9258
0.6350	8.7381	8.7396	9.9278	9.9258
0.6604	8.7373	8.7389	9.9284	9.9258
0.6858	8.7366	8.7381	9.9306	9.9266
0.7112	8.7371	8.7366	9.9306	9.9271
0.7366	8.7371	8.7368	9.9301	9.9266
0.7620	8.7386	8.7368	9.9284	9.9266
0.7874	8.7389	8.7363	9.9291	9.9273
0.8128	8.7394	8.7373	9.9314	9.9304
0.8382	8.7366	8.7340	9.9294	9.9304
0.8636	8.7394	8.7318	9.9235	9.9266
0.8890	8.7473	8.7335	9.9253	9.9273
0.9144	8.7429	8.7424	9.9289	9.9322
0.9398	8.7417	8.7368	--	9.9327

Table B-4. Cladding inside and outside diameter data for Rod 801-4

Distance from Bottom of Cladding (m)	Cladding Inside Diameter (mm)		Cladding Outside Diameter (mm)	
	0°	90°	0°	90°
0.0254	8.7490	8.7567	9.9055	9.9078
0.0508	8.7475	8.7541	9.9017	9.9146
0.0762	8.7536	8.7521	9.9304	9.9146
0.1016	8.7541	8.7457	9.9372	9.9408
0.1270	8.7533	8.7498	9.9327	9.9365
0.1524	8.7529	8.7462	9.9357	9.9380
0.1778	8.7533	8.7473	9.9388	9.9390
0.2032	8.7528	8.7490	9.9365	9.9347
0.2286	8.7495	8.7503	9.9388	9.9393
0.2540	8.7495	8.7521	9.9383	9.9362
0.2794	8.7531	8.7490	9.9360	9.9344
0.3048	8.7506	8.7508	9.9327	9.9357
0.3302	8.7495	8.7508	9.9337	9.9342
0.3556	8.7521	8.7465	9.9375	9.9344
0.3810	8.7485	8.7485	9.9322	9.9408
0.4064	8.7513	8.7437	9.9327	9.9395
0.4318	8.7511	8.7485	9.9322	9.9413
0.4572	8.7508	8.7498	9.9365	9.9281
0.4826	8.7452	8.7561	9.9372	9.9350
0.5080	8.7450	8.7556	9.9337	9.9319
0.5334	8.7470	8.7485	9.9352	9.9372
0.5588	8.7498	8.7490	9.9367	9.9383
0.5842	8.7498	8.7432	9.9365	9.9405
0.6096	8.7508	8.7485	9.9403	9.9507
0.6350	8.7523	8.7450	9.9372	9.9398
0.6604	8.7536	8.7511	9.9383	9.9352
0.6858	8.7495	8.7645	9.9459	9.9520
0.7112	8.7506	8.7500	9.9411	9.9294
0.7366	8.7539	8.7282	9.9190	9.9314
0.7620	8.7399	8.7394	9.9334	9.9418
0.7874	8.7452	8.7366	9.9339	9.9433
0.8128	8.7452	8.7371	9.9395	9.9365
0.8382	8.7455	8.7485	9.9428	9.9329
0.8636	8.7526	8.7417	9.9367	9.9339
0.8890	8.7465	8.7440	9.9370	9.9393
0.9144	8.7495	8.7437	9.9322	9.9383
0.9398	8.7485	8.7467	9.9344	--

Table B-5. Cladding inside and outside diameter data for Rod 801-5

Distance from Bottom of Cladding (m)	Cladding Inside Diameter (mm) 0°	Cladding Inside Diameter (mm) 90°	Cladding Outside Diameter (mm) 0°	Cladding Outside Diameter (mm) 90°
0.0254	8.7465	8.7574	9.9022	9.9162
0.0508	8.7442	8.7513	9.9022	9.9378
0.0762	8.7511	8.7432	9.9378	9.9484
0.1016	8.7533	8.7437	9.9375	9.9436
0.1270	8.7541	8.7391	9.9375	9.9433
0.1524	8.7539	8.7399	9.9385	9.9464
0.1778	8.7511	8.7409	9.9390	9.9418
0.2032	8.7478	8.7445	9.9357	9.9408
0.2286	8.7470	8.7401	9.9403	9.9411
0.2540	8.7488	8.7394	9.9370	9.9418
0.2794	8.7473	8.7414	9.9390	9.9393
0.3048	8.7414	8.7445	9.9390	9.9428
0.3302	8.7422	8.7450	9.9370	9.9446
0.3556	8.7442	8.7401	9.9378	9.9421
0.3810	8.7473	8.7442	9.9350	9.9438
0.4064	8.7457	8.7442	9.9337	9.9398
0.4318	8.7440	8.7450	9.9352	9.9418
0.4572	8.7462	8.7498	9.9365	9.9405
0.4826	8.7432	8.7462	9.9370	9.9413
0.5080	8.7432	8.7409	9.9383	9.9411
0.5334	8.7452	8.7406	9.9370	9.9413
0.5588	8.7473	8.7386	9.9383	9.9378
0.5842	8.7473	8.7406	9.9400	9.9375
0.6096	8.7460	8.7381	9.9413	9.9390
0.6350	8.7437	8.7396	9.9385	9.9378
0.6604	8.7427	8.7409	9.9367	9.9418
0.6858	8.7419	8.7429	9.9339	9.9428
0.7112	8.7409	8.7440	9.9350	9.9431
0.7366	8.7404	8.7434	9.9344	9.9411
0.7620	8.7376	8.7396	9.9400	9.9428
0.7874	8.7414	8.7389	9.9380	9.9449
0.8128	8.7386	8.7394	9.9423	9.9421
0.8382	8.7424	8.7366	9.9390	9.9423
0.8636	8.7409	8.7399	9.9372	9.9446
0.8890	8.7424	8.7396	9.9375	9.9400
0.9144	8.7404	8.7412	9.9367	9.9388
0.9398	--	--	9.9355	--

Table B-6. Fuel pellet physical characterization data for Rod 801-3

Pellet	Diameter (mm)	Length (mm)	Weight (g)	Immersion Density (g/cm^3)	Centerline Hole Diameter (mm)
1	8.5319	15.2438	8.4106	10.3821	0
2	8.5367	15.0731	8.3471	10.3975	0
3	8.5446	15.1966	8.4704	10.4096	0
4	8.5410	15.2215	8.4933	10.4429	0
5	8.5402	15.2425	8.4857	10.3837	0
6	8.5352	15.4031	8.5689	10.3989	1.8034
7	8.5405	15.3744	8.5574	10.3913	1.8034
8	8.5222	15.2016	8.4056	10.3606	1.8034
9	8.5408	15.1460	8.4217	10.3958	1.8034
10	8.5344	15.4242	8.5943	10.4310	1.8034
11	8.5408	15.2509	8.4574	10.3834	1.8034
12	8.5420	15.1648	8.4493	10.4196	1.8034
13	8.5344	15.1638	8.8300	--	0
14	8.5281	15.1618	8.7741	--	0
15	8.5420	15.0561	8.7639	10.4315	0
16	8.5441	15.4562	8.9714	--	0
17	8.5413	15.2639	8.8796	--	0
18	8.5364	15.2164	8.8539	--	0
19	8.5413	15.6990	8.5550	--	0
20	8.5392	15.5778	8.0530	--	0
21	8.5410	15.1409	8.8344	--	0
22	8.5443	15.1374	8.8208	--	0
23	8.5479	15.9913	8.7393	--	0
24	8.5443	15.7325	8.1745	--	0
25	8.5364	15.5214	8.0365	10.4124	0
26	8.5496	15.4953	8.0200	--	0
27	8.5458	15.1834	8.8488	--	0
28	8.5357	15.4155	8.9570	--	0
29	8.5509	15.2900	8.9030	--	0
30	8.5354	15.1508	8.7874	--	0
31	8.5392	15.3848	8.9768	--	0
32	8.5451	15.2151	8.8712	--	0
33	8.5453	15.8745	8.6554	--	0
34	8.5420	15.0353	8.7539	--	0
35	8.5225	15.9319	8.6675	10.4450	0
36	8.5372	15.0940	8.7564	--	0
37	8.5400	15.3063	8.9399	--	0
38	8.5476	15.3035	8.9392	--	0
39	8.5471	15.4046	8.9571	--	0
40	8.5491	15.4275	8.0014	--	0

Table B-6. (continued)

Pellet	Diameter (mm)	Length (mm)	Weight (g)	Immersion Density (g/cm^3)	Centerline Hole Diameter (mm)
41	8.5397	15.9098	8.7019	--	0
42	8.5474	15.4109	8.0227	--	0
43	8.5357	15.1559	8.8494	--	0
44	8.5468	15.6588	8.1387	--	0
45	8.5458	15.1049	8.7627	10.4140	0
46	8.5474	15.5009	8.0304	--	0
47	8.5476	15.4468	8.0154	--	0
48	8.5428	15.5118	8.0555	--	0
49	8.5420	15.0586	8.7864	--	0
50	8.5395	15.4102	8.9863	--	0
51	8.5425	15.3190	8.9443	--	0
52	8.5425	15.9804	8.7204	--	0
53	8.5420	15.3012	8.9094	--	0
54	8.5420	15.1511	8.8177	--	0
55	8.5463	15.2502	8.9035	10.4434	0
56	8.5519	15.2103	8.8337	--	0
57	8.5453	15.3391	8.9714	--	0
58	8.5418	15.2118	8.8020	--	0
59	8.5476	15.4056	8.9522	--	0
60	8.5390	15.4752	6.0920	--	0

dish shoulder of each pellet. Both diametral and length measurements were performed using a Bausch and Lomb optical gage, Model BR-25. The measurements were made with an accuracy of $\pm$0.005 mm. An analytical balance, accurate to $\pm$1 mg was used to obtain pellet mass and density data. Fuel pellet data for previously irradiated Rods 801-1 and 801-2 were unavailable, and the fuel pellet data used for unirradiated Rod 801-4 was unqualified, since the rod was irradiated in-pile only during the power calibration and preconditioning phase of the test.

The pretest void volumes for the previously irradiated rods were not recorded, but the design void volume of the rods (801-1 and 801-2) was 6×10^{-2} m^3. The pretest void volumes from previously unirradiated Rods 801-3, 801-4, and 801-5 are 8.2 $\pm$0.3, 5.7 $\pm$0.3, and 5.6 $\pm$0.3 $\times 10^{-2}$ m^3, respectively. The somewhat larger void volume of Rod 801-3 was

Table B-7. Fuel pellet physical characterization data for Rod 801-5

Pellet	Diameter (mm)	Length (mm)	Weight (g)	Immersion Density (g/cm^3)	Centerline Hole Diameter (mm)
1	8.5362	15.1351	8.7802	--	0
2	8.5314	15.0807	8.7992	--	0
3	8.5402	15.1051	8.8345	--	0
4	8.5441	15.4043	9.0332	--	0
5	8.5405	15.4671	9.0327	10.4514	0
6	8.5369	15.3721	8.9950	--	0
7	8.5405	15.1031	8.8239	--	0
8	8.5372	15.1437	8.8100	--	0
9	8.5441	15.2974	8.9638	--	0
10	8.5471	15.2679	8.9459	--	0
11	8.5453	15.1021	8.8255	--	0
12	8.5339	15.3647	8.9951	--	0
13	8.5392	15.2039	8.8443	--	0
14	8.5443	15.1658	8.9004	--	0
15	8.5349	15.1105	8.8101	10.4281	0
16	8.5364	15.1897	8.8934	--	0
17	8.5415	15.2651	8.9355	--	0
18	8.5380	15.3373	8.9796	--	0
19	8.5357	15.2984	8.9480	--	0
20	8.5402	15.4615	9.0480	--	0
21	8.5395	15.3198	8.9565	--	0
22	8.5362	15.3286	8.9608	--	0
23	8.5385	15.2408	8.9134	--	0
24	8.5369	15.2847	8.9331	--	0
25	8.5397	15.5019	9.0593	10.4411	0
26	8.5395	15.2075	8.9008	--	0
27	8.5377	15.3960	9.0010	--	0
28	8.5374	15.0734	8.7665	--	0
29	8.5430	15.1719	8.8775	--	0
30	8.5420	15.1854	9.0395	--	0
31	8.5397	15.0924	8.8250	--	0
32	8.5298	15.2530	8.9169	--	0
33	8.5395	15.2786	8.9160	--	0
34	8.5319	15.2458	8.8625	--	0
35	8.5413	15.1628	8.8685	10.4589	0
36	8.5410	15.1191	8.8122	--	0
37	8.5410	15.4818	9.0339	--	0
38	8.5354	15.2672	8.9224	--	0
39	8.5397	15.9591	8.7338	--	0
40	8.5410	15.2580	8.8762	--	0

Table B-7. (continued)

Pellet	Diameter (mm)	Length (mm)	Weight (g)	Immersion Density (g/cm^3)	Centerline Hole Diameter (mm)
41	8.5425	15.2728	8.9022	--	0
42	8.5402	15.4026	8.9811	--	0
43	8.5344	15.4300	8.9796	--	0
44	8.5316	15.1498	8.8560	--	0
45	8.5377	15.1712	8.8353	10.4197	0
46	8.5369	15.2730	8.9332	--	0
47	8.5341	15.2037	8.8230	--	0
48	8.5514	15.3916	9.0179	--	0
49	8.5339	15.1638	8.8362	--	0
50	8.5471	15.0851	8.8280	--	0
51	8.5466	15.1717	8.8829	--	0
52	8.5329	15.2687	8.9024	--	0
53	8.5395	15.3114	8.9260	--	0
54	8.5344	15.1089	8.8276	--	0
55	8.5413	15.4610	9.0632	10.4673	0
56	8.5392	15.5138	9.0772	--	0
57	8.5418	15.0805	8.8083	--	0
58	8.5496	15.2519	8.8770	--	0
59	8.5364	15.2883	8.9157	--	0
60	8.5499	10.6655	6.2049	--	0

accounted for by the presence of 12 fuel pellets in the fuel column containing centerline holes to contain the fuel thermocouple. The top end cap of Rod 801-1 was removed and replaced with an end cap containing a pressure transducer. The rod was prepressurized with a mixture of 77.7% helium and 22.3% argon gases at ambient temperature to 0.103 MPa. This gas mixture approximates the thermal conductivity of the fill gas in an irradiated fuel rod. Rod 801-2 was not opened prior to testing and contained its initial inventory of air plus fission gases at about 0.103 MPa. Previously irradiated Rods 801-3, 801-4, and 801-5 were backfilled at ambient temperatures with a commercially pure helium gas to pressures of 0.103 MPa each. The upper end cap of Rod 801-3 was replaced with an end cap containing an internal pressure transducer, plenum thermometer, and centerline fuel thermocouple. The top 12 fuel pellets in the fuel column (between 0.740

and 0.914 m from the bottom of the fuel stack) were replaced with fuel pellets containing 1.8-mm-diameter drill holes to accommodate insertion of the fuel centerline thermocouple.

2. CLADDING TEXTURE CHARACTERIZATION

The thermal-mechanical processing of zircaloy into tubing produces a strong crystallographic texture. Typically, the commonly observed texture is a bimodal distribution of basal poles concentrated in the radial-to-tangential plane of the tube. The strong crystallographic texture produces a pronounced anisotropy in the mechanical properties of the tubing. A wide range of textures may be found, depending on the manufacturing process. In the following sections, the nominal crystallographic texture of the Saxton cladding used in the Test RIA 1-1 fuel rods is characterized, and the plastic behavior of the cladding is analyzed.

The crystallographic texture of the irradiated Saxton tubing was determined by inverse pole figure techniques from X-ray diffraction data. Measurement of the integrated intensities, {I}, of diffraction peaks from a sample allowed construction of a contour map (inverse pole figure) using the ratio of intensities, $\{I:I_o\}$, assigned to appropriate orientations in the standard projection, as shown in Figure B-1, for the (0001) standard projection of α zircaloy.[B-2,B-3] The angle ϕ shows the extent of tilt of the diffracting plane's pole from the basal pole (0001). The angle α shows the plane's rotation about the basal pole. Crystallographic planes lying parallel to the plane of the sample surface will contribute to the measured diffracted intensity for a scan at the Bragg angle, ϕ. The preferred orientation in basal poles is then obtained from the orientation distribution function of intensities in the diffractometer pattern.

The inverse pole figures for the tangential (t), radial (r), and axial directions typical to the Saxton cladding are shown in Figure B-2 (insets a, b, and c, respectively), for the unirradiated cladding (inset d), and for the axial direction in the previously irradiated cladding.[B-1] The (0001) basal poles lie in both the radial and tangential directions, with about 45% of the poles lying in the tangential direction. The nominal

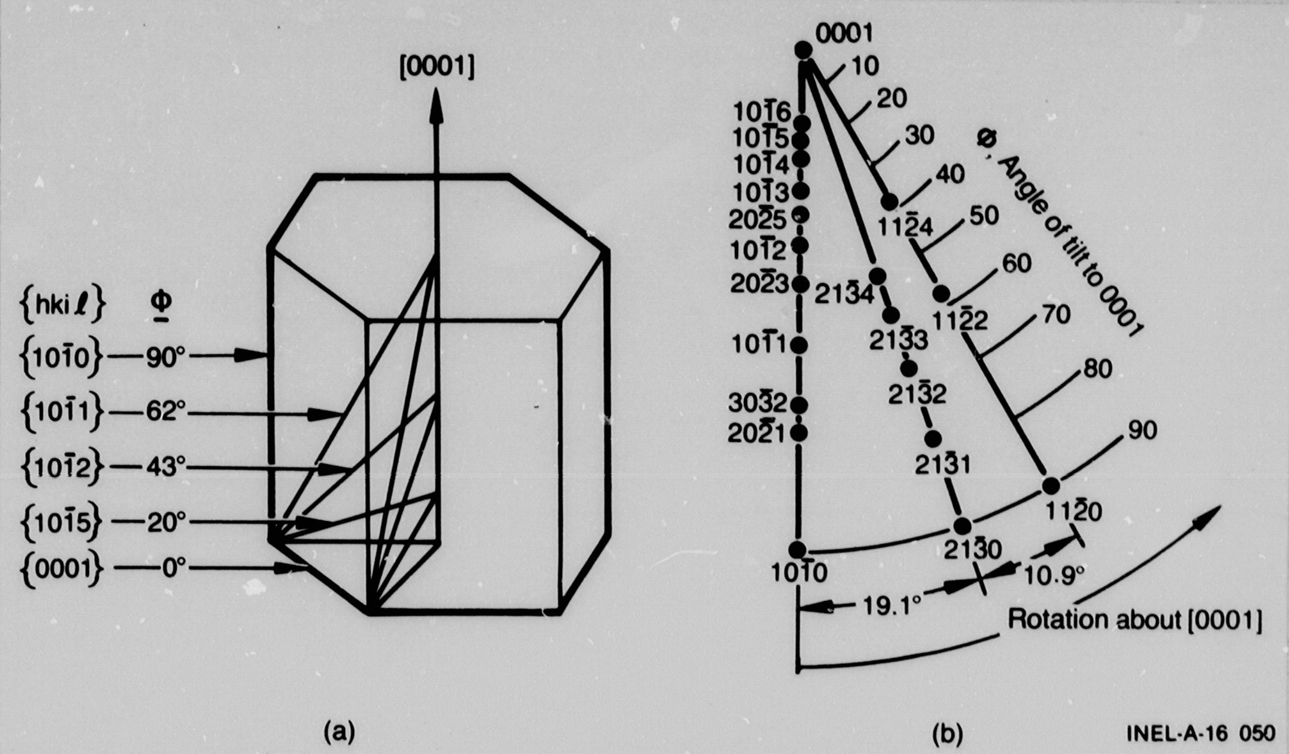

Figure B-1. Schematic relationship of (a) the tilt (ϕ) between {0001} and conjugate planes {h, k, i, l}, illustrated for {$10\bar{1}\ell$}, and (b) the standard projection of diffracting planes for α phase zirconium, c/a = 1.59.

normalized weighted average of the basal poles in these samples is $F \gtrsim 0$ (ϕ is slightly > 45-degrees) in the r-to-t plane of the tube.[a] A large number of the ($10\bar{1}0$) and ($11\bar{2}0$) poles lie in the axial direction. Since the ($10\bar{1}0$) and ($11\bar{2}0$) texture coefficients in the axial direction are about double the value of the coefficient of the (0001) pole in either the radial or tangential directions, each of the basal orientations could contribute to ($10\bar{1}0$) or ($11\bar{2}0$) orientation in the axial direction.[B-4] Possible orientations of the basal poles are illustrated in Figure B-3.

The orientation parameter, f, for a given reference direction relates the materials properties to the degree of physical isotropy. The f parameter for the Saxton cladding was evaluated for f_r, denoting the radial

---

a. The normalized weighted average of basal poles in the r-to-t plane of the tube, texture factor F, range from F = 1 when all basal poles are oriented radially, to F = -1 when all the basal poles are oriented tangentially. When all the basal poles are equally distributed about the 45-degree direction, F = 0.

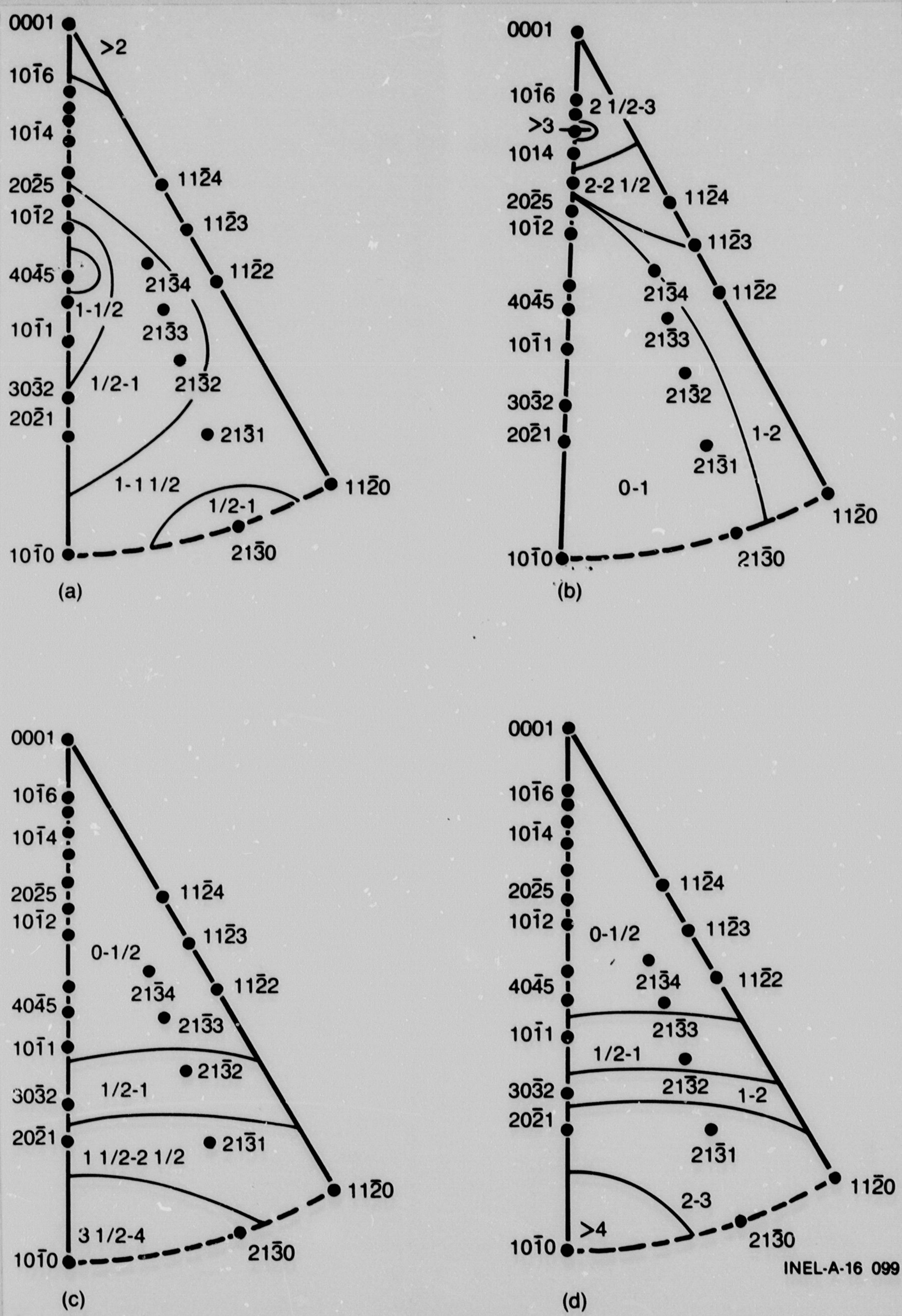

Figure B-2. **Pole figures for Saxton cladding (a) unirradiated tangential direction, (b) unirradiated radial direction, (c) unirradiated axial direction, and (d) irradiated axial direction.**

FORM EG&G-376
(Rev 04-79)

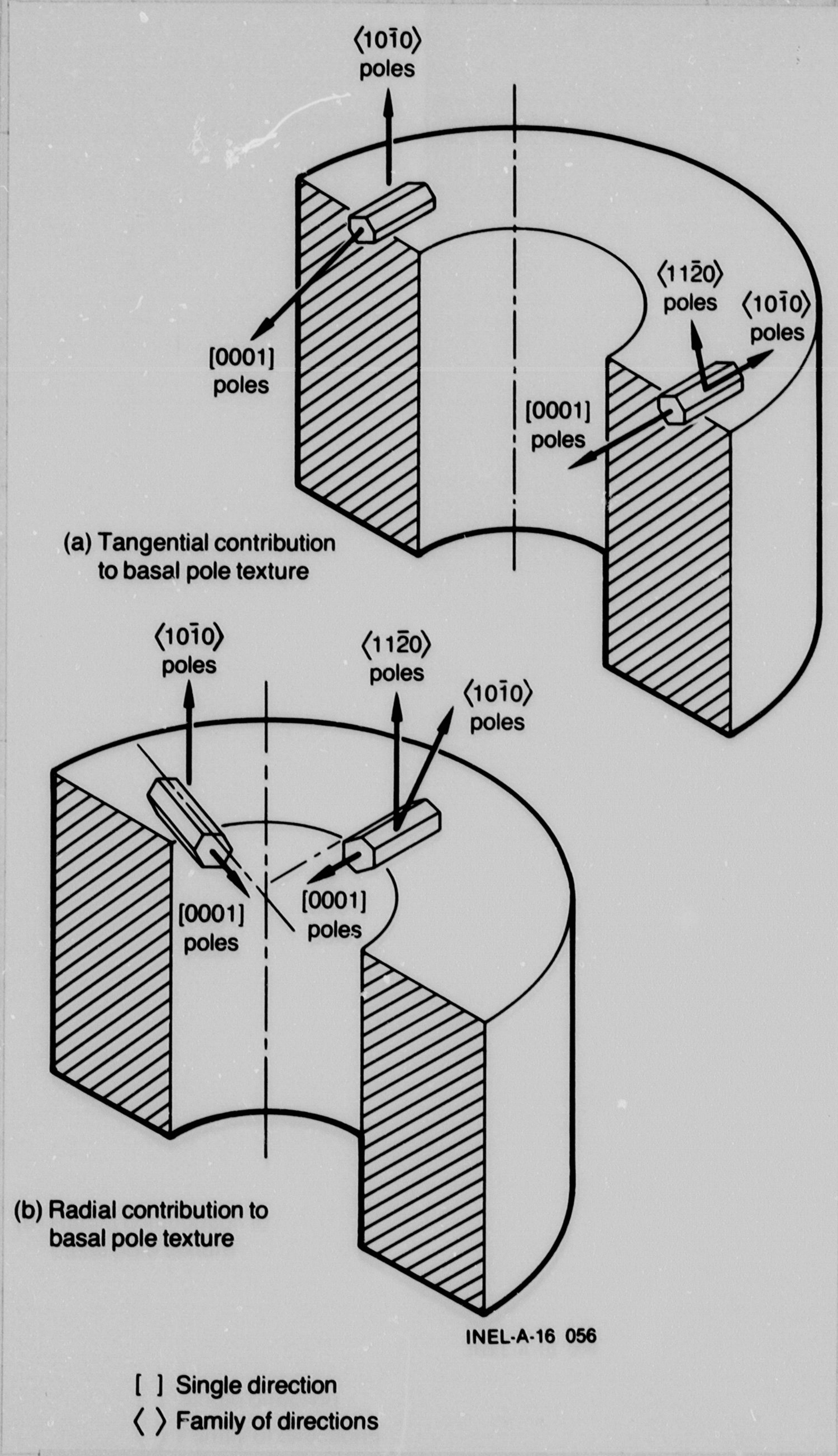

Figure B-3. Orientation of unit cells for different textures in Saxton tubing.

direction of the tubing. The radial orientation of basal poles over the stereogram nominally ranged to $f_r \gtrsim 1/2$,[a] suggesting a mixture of orientations present. Although not measured, the expected contractile strain ratio, R, for the Saxton tubing deformed axially in tension, is R ∿ 1:2.

The texture coefficients in the axial direction indicated that some grains underwent a 30-degree rotation of the (11$\bar{2}$0) poles about the c-axis so that some of the (10$\bar{1}$0) poles lie in the axial direction as a result of the fabrication. Evidence of residual cold work in the axial direction in the Saxton tubing is seen from the ratio of texture coefficients in the (10$\bar{1}$0) and (11$\bar{2}$0) directions, which is > 1 [the (1010) texture coefficient is 3.95, compared with the (1120) coefficient of 2.32, with the ratio (1010) being 1.70].[B-5]

The coefficients obtained in the axial direction for irradiated cladding exhibited only slightly larger values of the texture coefficients for (10$\bar{1}$0) and (11$\bar{2}$0) poles, compared with unirradiated cladding values. The comparison suggests that no significant changes occurred in the tubing texture as a result of the Saxton irradiation.

From the available data, an approximate pole figure representative of the Saxton cladding was constructed, showing the basal pole texture, and is presented in Figure B-4. The corresponding von Mises yield locus representing the yield strength anisotropy is sketched below the pole figure. The basal pole intensity maxima are near, but slightly greater than, 45 degrees in the r-to-t plane.

The zircaloy deforms primarily by prismatic plane slip for temperatures up to about 680 to 780 K.[B-6] Basal pole deformation occurs by twinning. Although a variety of twinning modes exist, the resolved shear stress required for twinning is greater than the resolved shear stress for slip. Tube textures indicating a direction with a large concentration of

---

a. Alignment of the basal poles perpendicular or parallel to the radial direction varies from $0 \le f_r \le 1$, respectively. Basal poles equally distributed about 45 degrees from the radial direction give a value $f_r = 1/2$, and physically isotropic, $f_r = 1/3$.

FORM EG&G-376
(Rev. 04-79)

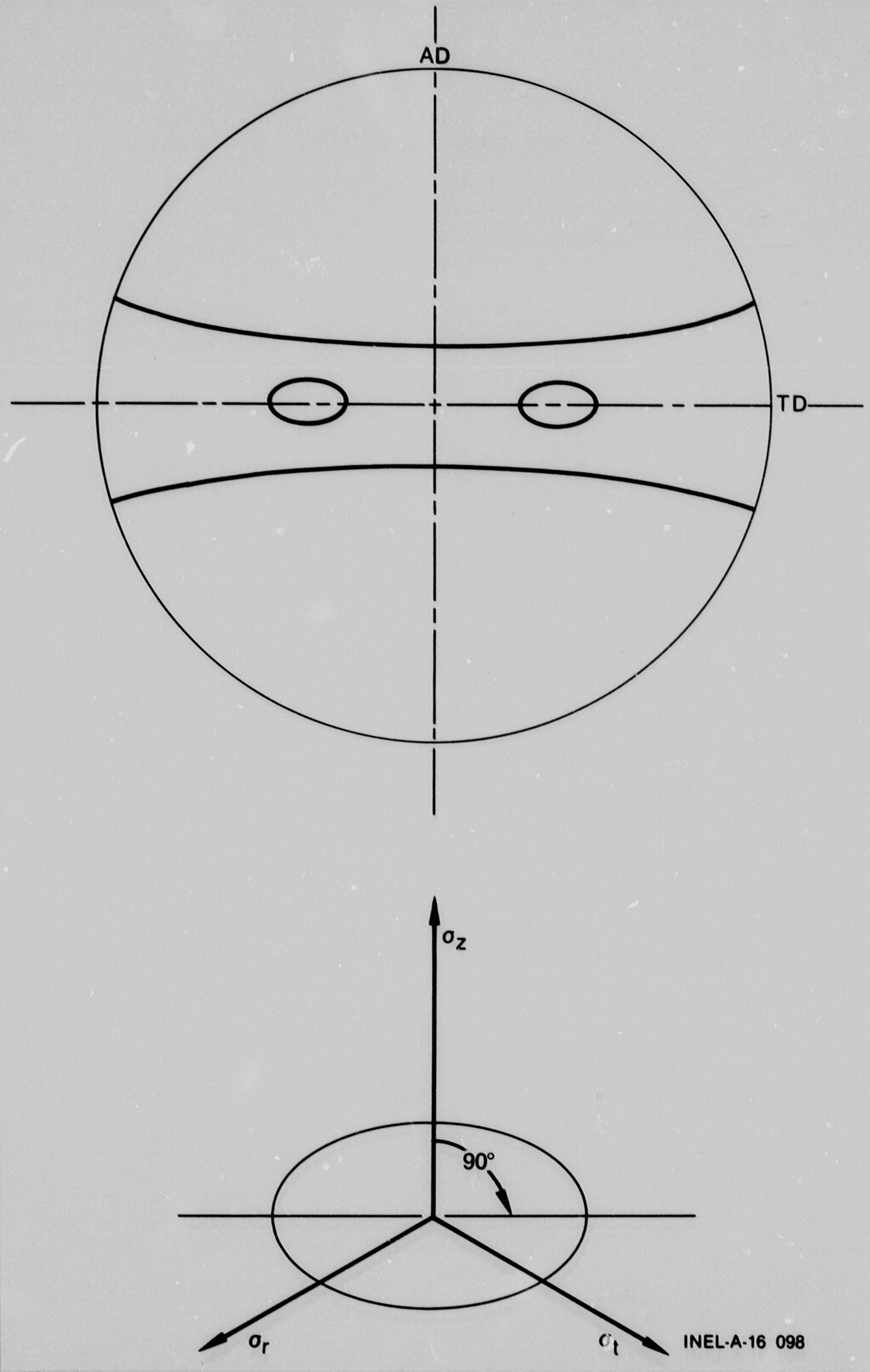

Figure B-4. Saxton tube basal pole texture and corresponding yield loci representing the mechanical anistropy of the yield strength.

basal poles will tend to resist deformation along that direction. The Saxton rod deformation texture has a tendency for more basal poles to be aligned in the radial direction (F slightly > 0); therefore, deformation in the tangential direction would be slightly more favorable than in the radial direction, but nearly equal amounts of tangential and radial deformation may occur.

Since deformation by basal pole twinning is energetically less favorable than prismatic slip, it is assumed that all of the plastic deformation occurring in the Saxton cladding would be by either prismatic slip, in a directon perpendicular to the axial direction (c axis of the hexagonal grains), or dislocation slip, representative of twinning modes. Preferred radial positioning of the basal poles leads to a condition of high hoop resistance. Axial loading with active, radially aligned basal poles produces elongation by diameter reduction, with little change in wall thickness, whereas active tangentially aligned basal poles produce elongation by decreasing wall thickness, with little change in diameter.[B-5]

3. REFERENCES

B-1. G. W. Gibson et al., Characteristics of UO_2-Zircaloy Fuel Rod Materials from the Saxton Reactor for Use in the Power Burst Facility, ANCR-NUREG-1321, September 1976.

B-2. J. J. Kearns, Thermal Expansion and Preferred Orientation in Zircaloy, WAPD-TM-472, November 1965.

B-3. L. F. P. Van Swam et al., "Relationship Between Contractile Strain Ratio R, and Texture in Zirconium Alloy Tubing," Metallurgical Transactions, A 10A, 1979, pp. 483-487.

B-4. C. R. Woods et al., Properties of Zircaloy-4 Tubing, WAPD-TM-585, 1966.

B-5. E. Tenckhoff and P. L. Rittenhouse, "Annealing Textures in Zircaloy Tubing," Journal of Nuclear Materials, 35, 1970, pp. 14-23.

B-6. E. Tenckhoff, "Operable Deformation Systems and Mechanical Behavior of Textured Zircaloy Tubing," Zirconium in Nuclear Applications, ASTM STP 552, American Society for Testing and Materials, August 1974, pp. 179-200.